DOI: 10.1002/ejic.200500693

Spectroscopic Comparison of Dinuclear Ti^{+} and Ti^{2+} μ-η¹:η¹ Dinitrogen Complexes with Cp*/Pentafulvene and Amine/Amide Ligation: Moderate versus Strong Activation of N_2

Felix Studt,[a] Nicolai Lehnert,[a] Beatrix E. Wiesler,[a][‡] Axel Scherer,[b] Rüdiger Beckhaus,*[b] and Felix Tuczek*[a]

Keywords: Metallocenes / Nitrogen fixation / Titanium / Raman spectroscopy / Density functional calculations

The two dinuclear, end-on dinitrogen-bridged titanium complexes with cp*/pentafulvene ligation, [{(η^5-C_5Me_5)Ti(η^6-$C_5H_4CR_2$)}$_2$(μ-η^1:η^1-N_2)], R = *p*-tolyl (**1**) and >CR_2 = adamantylidene (**2**), are compared to an analogous titanium dinitrogen complex with a mixed amine/amide/chloride ligand set, [{($Me_3Si)_2$NTiCl(TMEDA)}$_2$(μ-η^1:η^1-N_2)] (**3**; TMEDA = tetramethylethylenediamine). The N–N stretching vibrations of complexes **1** and **2** are observed at 1749 and 1755 cm^{-1}, respectively, indicative of a moderate activation of the dinitrogen ligand. In contrast, the N–N stretch of **3** is located at 1284 cm^{-1}, reflecting a much more highly activated N_2 ligand. These findings are in qualitative agreement with N–N bond lengths that have been observed experimentally. DFT calculations reveal that the major difference in the electronic structures of **1**, **2**, and **3** is the fact that only one of the N_2 π* orbitals is (doubly) occupied in the case of **1** and **2**, whereas both π* orbitals are (doubly) occupied in the case of **3**. The reason for this finding is that in **1** and **2** two of the three electrons of each Ti^{+} are involved in back-bonding interactions with the terminal fulvene ligands, whereas no such interactions exist between the Ti^{2+} centers of **3** and its terminal set of donor ligands.

Introduction

The bonding and activation of N_2 by early transition-metal complexes is of continued interest.[1–4] In titanium systems dinitrogen is usually coordinated in an end-on bridging geometry.[5] The activation of the N_2 ligand can generally be determined by considering N–N bond lengths obtained from X-ray diffraction data and N–N stretching frequencies obtained from vibrational spectroscopy. These data allow titanium dinitrogen compounds to be divided into moderately and strongly activated species.[6] Moderately activated dinitrogen complexes are generally found for titanocene-based systems with N–N bond lengths in the range of 1.15–1.20 Å.[7–12] Strong activation, on the other hand, is observed for titanium complexes with ligand sets that are different from cyclopentadienyl, exhibiting N–N bond lengths of 1.25–1.30 Å.[13–15] A collection of N–N bond lengths of different dinitrogen complexes is given in Table 1. The two complexes with cp*/pentafulvene ligation, [{(η^5-C_5Me_5)Ti(η^6-$C_5H_4CR_2$)}$_2$(μ-η^1:η^1-N_2)], R = *p*-tolyl (**1**) and >CR_2 = adamantylidene (**2**), both have N–N bond lengths of 1.160 Å and thus can be considered to be moderately activated.[7] On the other hand, the complex [{($Me_3Si)_2$-NTiCl(TMEDA)}$_2$(μ-η^1:η^1-N_2)] (**3**; TMEDA = tetramethylethylenediamine) that exhibits a mixed amine/amide/chloride set of coligands has an N–N bond length of 1.29 Å and therefore activates N_2 to a higher degree (cf. Scheme 1).[13] This would indicate that the activation of N_2 is higher in compound **3**, formally a Ti^{2+}–Ti^{2+} species, than in compounds **1** and **2**, formally Ti^{+}–Ti^{+} complexes. At first sight this observation appears to be contradictory.

Table 1. Comparison of N–N bond lengths of different dinitrogen complexes.

Compound	N–N bond lengths [Å]	Ref.
1	1.160(3)	[7]
2	1.160(5)	[7]
[{(η^5-$C_5Me_5)_2$Ti}$_2$(μ-η^1:η^1-N_2)]	1.165(14)	[8]
[{(η^5-$C_5Me_4H)_2$Ti}$_2$(μ-η^1:η^1-N_2)]	1.170(4)	[9]
[{(η^5-$C_5H_5)_2$Ti(PMe_3)}$_2$(μ-η^1:η^1-N_2)]	1.191(8)	[10]
[{(η^5-$C_5H_5)_2$Ti(*p*-tolyl)}$_2$(μ-η^1:η^1-N_2)]	1.162(12)	[11]
[{[η^5-$C_5H_3(SiMe_3)_2]_2$Ti}$_2$(μ-η^1:η^1-N_2)]	1.164(5)	[12]
3	1.289(9)	[13]
[{($Me_3Si)_2$NTiCl($py)_2$}$_2$(μ-η^1:η^1-N_2)]	1.263(7)	[14]
[{[(Me_2N)C(N*i*Pr)$_2]_2$Ti}$_2$(μ-η^1:η^1-N_2)]	1.280(8)	[15]

In order to address the above statement we investigated compounds **1**, **2**, and **3** with resonance Raman spec-

[a] Institut für Anorganische Chemie, Christian-Albrechts-Universität Kiel,
24098 Kiel, Germany
E-mail: ftuczek@ac.uni-kiel.de
[b] Institut für Reine und Angewandte Chemie, Fakultät für Mathematik und Naturwissenschaften, Carl von Ossietzky Universität Oldenburg,
Postfach 2503, 26111 Oldenburg, Germany
E-mail: ruediger.beckhaus@uni-oldenburg.de
[‡] Present address: Merck KGaA, Darmstadt

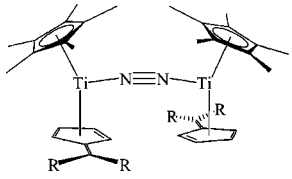

R = *p*-Tol (1)

>CR_2 = adamantylidene (2)

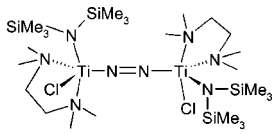

(3)

Scheme 1.

troscopy. The vibrational analysis was assisted by DFT calculations performed on structures **I** and **III**, which are models of complexes **1/2** and **3**, respectively. The UV/Vis spectra of **1/2** and **3** were interpreted on the basis of MO schemes of models **I** and **III**. The electronic-structural features leading to the observed differences in N_2 activation were identified through this combined spectroscopic-theoretical approach. The general implications of this result are discussed below.

Results and Analysis

Vibrational Spectra and Analysis

Solid-state resonance Raman spectra of complexes **1**–**3**, recorded with an excitation wavelength of 514.5 nm, are shown in Figure 1. The most intense peak in the Raman spectrum of **1** is located at 1749 cm^{-1}. This feature is assigned to the N–N stretching mode of the Ti–N_2–Ti unit on the basis of its high intensity and energetic position. The first and second overtones of this mode are found at 3475 and 5173 cm^{-1}, respectively. In the Raman spectrum of **2** the N–N stretching mode is identified at 1755 cm^{-1} by the same arguments. The overtones are located at 3490 and 5185 cm^{-1}. The most prominent feature in the Raman spectrum of **3** is observed at 1284 cm^{-1}. Again, this peak is assigned to the N–N stretching frequency of the Ti–N_2–Ti unit because of its high intensity and energetic position.

DFT calculations were performed for structures **I** and **III**. In structure **I** the ligands of **1** and **2** are replaced by

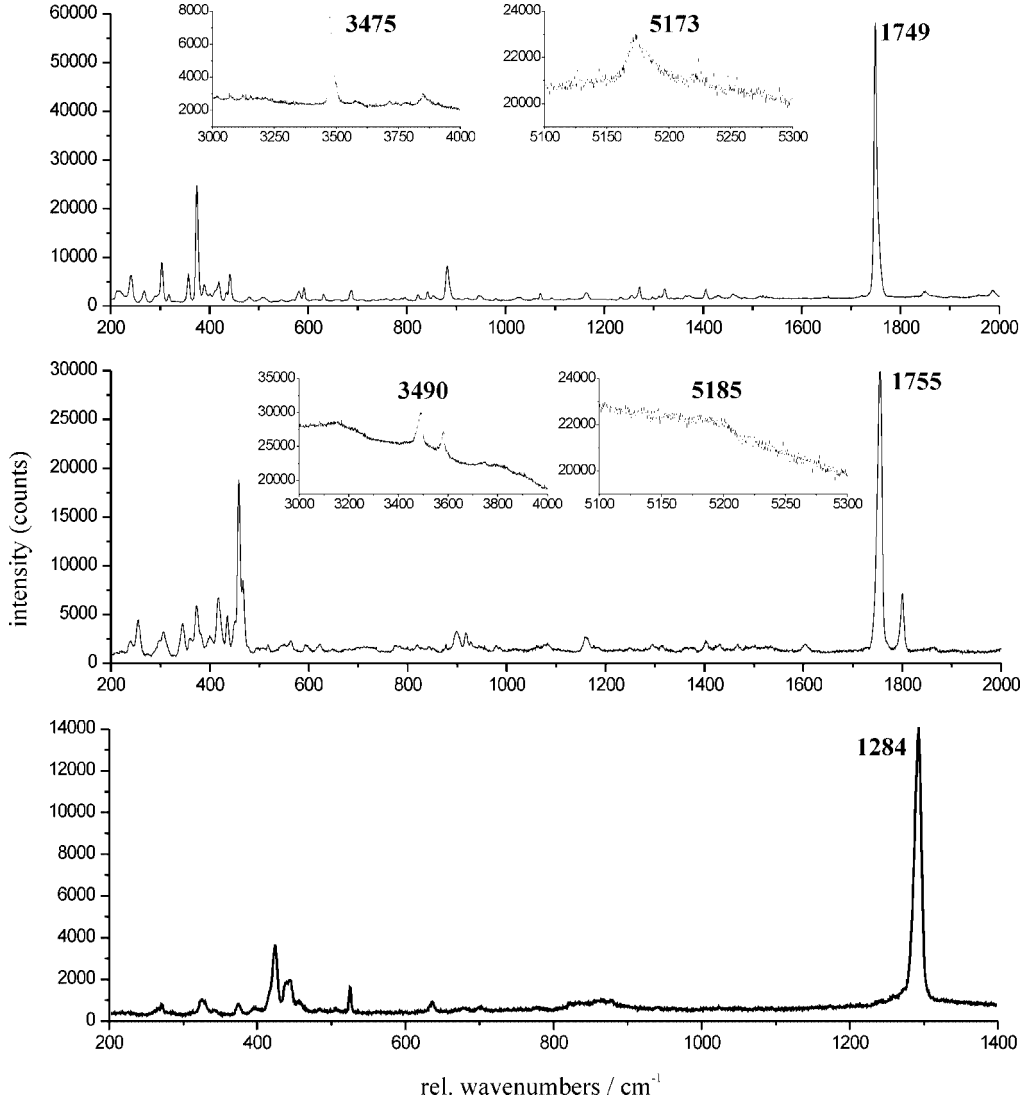

Figure 1. Top: Raman spectrum of **1**. Middle: Raman spectrum of **2**. Bottom: Raman spectrum of **3**. All Raman spectra were recorded with an excitation wavelength of 514.5 nm.

unsubstituted cyclopentadienyl and fulvene groups, thus providing a model system for both complexes **1** and **2**. Note, however, that in model **I** the dihedral angle between the Ct*–Ti vectors of the two halves of the dimers is approximately zero (Ct* is the center of the cp* ligand). This reproduces the structure of complex **1** but not that of complex **2**, which exhibits a twisted configuration (dihedral angles between the Ct*–Ti vectors are 19.1° and 20.0°, respectively, for the two independent molecules in the asymmetric unit). Model **III** has been simplified with respect to complex **3** by approximating the TMEDA and $(Me_3Si)_2N$ ligands through coordinated NH_3 and NH_2 groups, respectively. Structural parameters resulting from the DFT geometry optimizations are compared with the experimental values in Table 2; a comparison between the experimentally determined frequencies (see above) and the values derived from DFT (B3LYP) is given in Table 3. The calculated frequencies qualitatively reproduce the experimentally observed trend. The N–N stretching frequency of **I** is calculated at 1806 cm^{-1}, in good agreement with the experimentally determined value of 1749 cm^{-1}. The N–N stretching mode of the model complex **III** is theoretically predicted to be at a much lower energy (1371 cm^{-1}), in fair agreement with the corresponding peak in the Raman spectrum of **3** (1284 cm^{-1}). In this case the larger deviation from the experimental data probably results from the greater simplification of the terminal ligands employed in the calculation.

Table 2. Comparison of structural parameters of **1**, **2**, and **I**.

Complex	N–N	Ti–N	Ti–Ct*	Ti–Ct^{Fv}	Ti–N–N	θ
1	1.160	1.999	2.056	1.965	170.0	28.3
2	1.160	2.008	2.064	1.986	169.8	31.6
I	1.204	1.916	2.087	2.043	176.9	35.7

Table 3. Comparison of the observed and calculated frequencies of complexes **1**–**3** with model systems **I** and **III**.

Mode	Experimental			B3LYP	
	1	**2**	**3**	**I**	**III**
ν_{NN}	1749	1755	1284	1806	1371
2 ν_{NN}	3475	3490	–	–	–
3 ν_{NN}	5173	5185	–	–	–

Electronic Structure

An understanding of the electronic structure of complexes **1/2** and complex **3** is achieved on the basis of the MO schemes of the corresponding models **I** and **III**, respectively (Figure 2). Model **I** is oriented such that the *x* axis is directed along the N–N vector and the *y* axis along the fulvene/cyclopentadienyl ligands. Figure 2 (left) shows contour plots of important molecular orbitals of **I**. The HOMO of **I** represents a bonding combination between the π_z* orbital of dinitrogen and the metal d_{xz} orbitals, forming a metal–dinitrogen π bond; this orbital has nearly equal contributions from the nitrogen p orbitals and the d functions of titanium. The LUMO of **I** is the bonding combination of the N_2 π_y* orbital and the metal d_{xy} functions. The corresponding orbital has 19% metal and 40% nitrogen character. The LUMO+1 of **I** is an antibonding combination of the metal d_{xz} orbitals with the dinitrogen π_z orbital having 6% nitrogen character. As only one π* orbital of the dinitrogen ligand is occupied, the N_2 ligand has been formally reduced by the Ti^{+} centers of **I** to an N_2^{2-} oxidation state. The remaining electrons of the two titanium atoms are located in the two sets of d_{z^2} orbitals (in-phase and out-of-phase combinations) both of which interact in a bonding fashion with fulvene π* orbitals to form two d_{z^2}_Fv orbitals. Both MOs have 61% fulvene character, indicative of a significant back-bonding from the metals to the fulvene ligands.

Model **III** is also oriented such that the *x* axis is along the N–N vector; the *y* axis lies in the plane of the paper, between the amino and amido ligands on the one side and the amido and chloro ligands on the other side of the dinuclear complex. The π* orbitals of the dinitrogen ligand (π^*_z and π^*_y) form the two dinitrogen–metal π bonding combinations π^*_z_d_{xz} and π^*_y_d_{xy}, respectively, which have nearly equal charge contributions from dinitrogen and metal d functions (Figure 2, right). Both of these orbitals are now occupied, corresponding to the HOMO–1 and the HOMO of **III**, respectively. Model **III** therefore has two metal–dinitrogen π bonds, and the dinitrogen ligand of **3** is formally reduced by its two Ti^{2+} centers to a (–4) charge state. In Figure 2 the orbitals of **I** and **III** are arranged in a way that clarifies the relationship between the electronic structures of **1/2** and **3**. Evidently, the dinitrogen parts of the frontier orbitals are very similar; the major difference between the two systems lies in the fact that both π* orbitals of dinitrogen are occupied for **3**, whereas for **1** and **2** one dinitrogen π* orbital (the HOMO) is occupied and the other (the LUMO) is empty.

Table 4 summarizes the atomic charges obtained for models **I** and **III** by natural population analysis (NPA). As already inferred from the preceding orbital analysis, a significant amount of electronic charge is transferred from the titanium centers of both **I** and **III** to the bridging dinitrogen ligand. However, the negative charge on this ligand is much larger for **III** (–0.80) than for **I** (–0.24), in qualitative agreement with the fact that both π* orbitals of N_2 are occupied in **III** whereas only one π* orbital is occupied in **I**. As the π^*_d_π orbitals of **I** and **III** have roughly equal contributions from the metal d orbitals and the dinitrogen π* functions, the formal charges of –2 and –4 are approximately halved, leading to approximate descriptions of the N_2 ligand as N_2^{1-} in **1/2** and N_2^{2-} in **3**. The actual charges determined by NPA (–0.24 for **I** and –0.80 for **III**; vide supra) reflect a further charge donation from lower-energy π and σ bonding orbitals of N_2 back into the unoccupied metal d orbitals. The titanium atoms, in turn, are calculated to have charges of +0.34 for model **I** and +1.00 for model **III**, in qualitative agreement with the different formal oxidation states obtained after interaction with N_2 (Ti^{2+} for **I** and

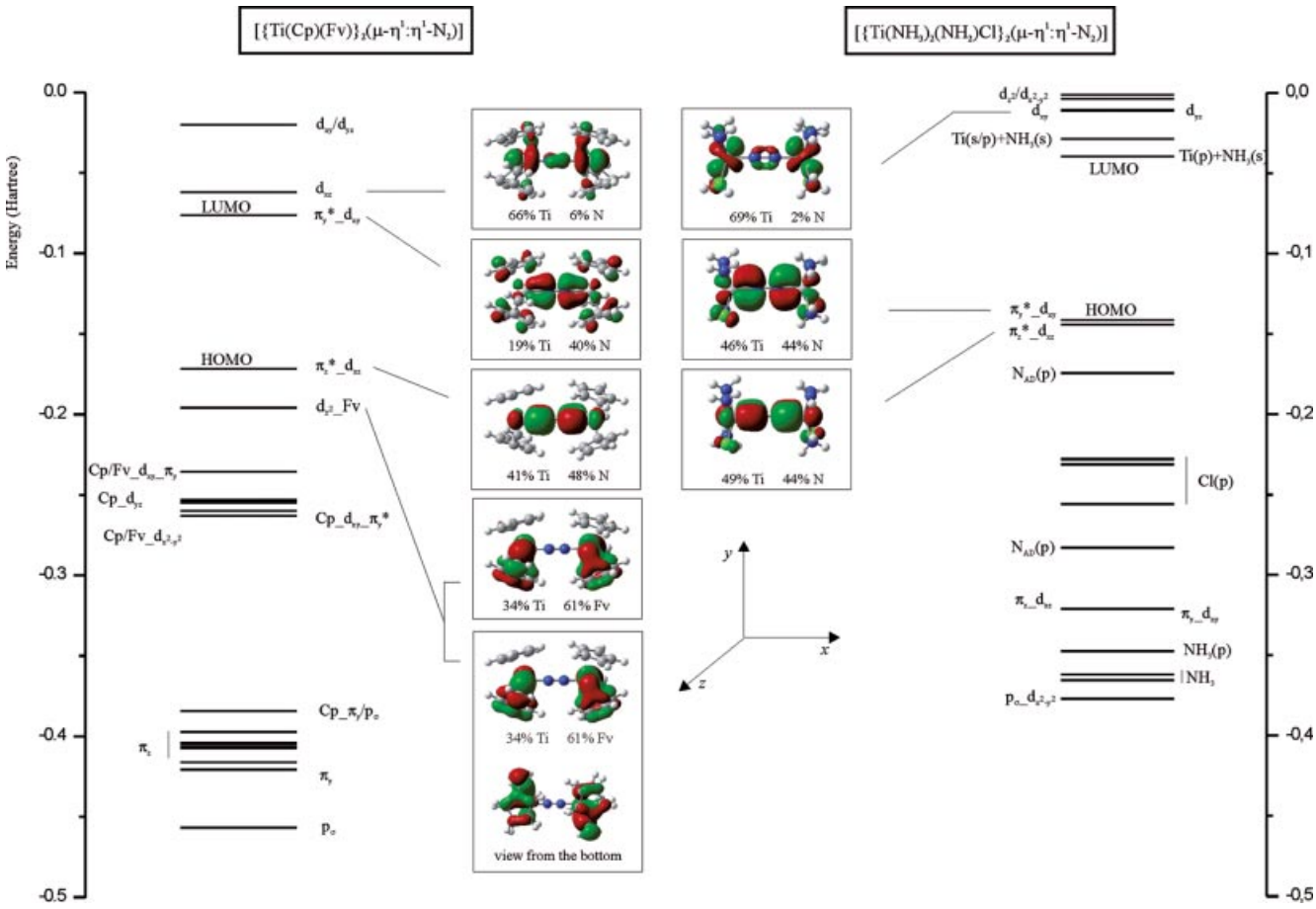

Figure 2. MO diagram of models **I** and **III** together with contour plots of important molecular orbitals of **I** and **III**.

Ti^{4+} for **III**). The actual charges on the metal atoms are further influenced by donor/acceptor interactions with the terminal ligands. It can be inferred from Table 4 that the cp* ligands of **I** donate 0.93 charge units to the metal centers (resulting charge –0.07), whereas the (formally neutral) fulvene ligands act as charge acceptors (resulting charge –0.16).

Table 4. NPA charges of model systems **I** and **III**.

Complex	Atom						
	Ti[a]	N[a]	Cp[b]	Fu[b]	NH_3[b]	NH_2[b]	Cl[a]
I	0.34	–0.12	–0.07	–0.16	–	–	–
III	1.00	–0.40	–	–	0.15	–0.39	–0.51

[a] Charge for each atom. [b] Charge for the corresponding ligand.

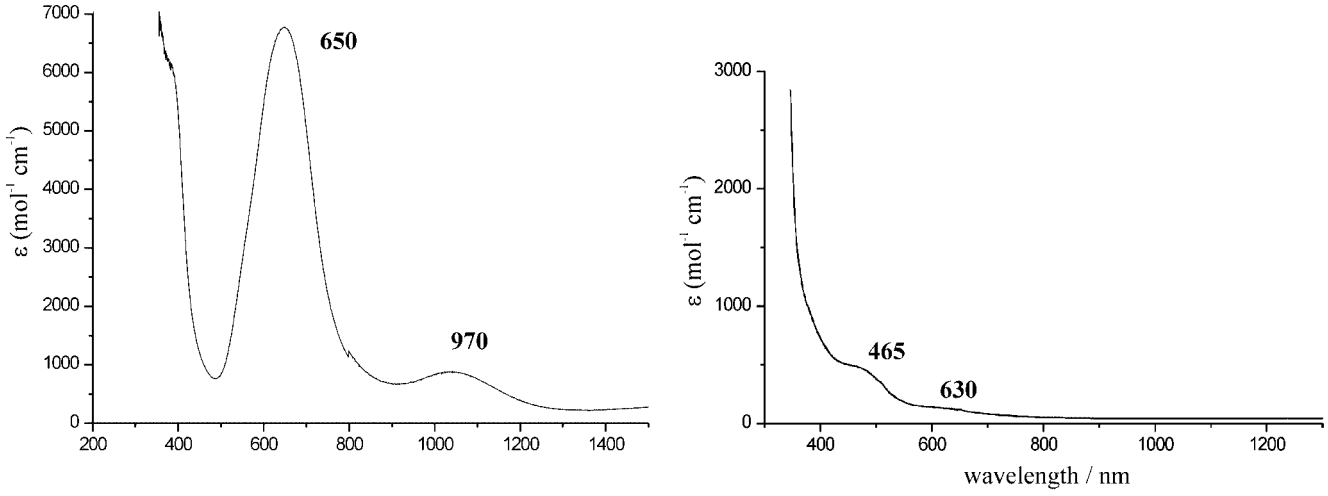

Figure 3. UV/Vis spectrum of **2** (left) and **3** (right).

UV/Vis Spectroscopy

The UV/Vis spectra of **1** and **2** are very similar. The absorption spectrum of **2** (Figure 3, left) exhibits two bands at 970 (ε = 900 $M^{-1}cm^{-1}$) and 650 nm (ε = 6700 $M^{-1}cm^{-1}$). As there is no band at lower energies, the 970-nm band is assigned to the lowest energy transition of **2**, which corresponds to the HOMO–LUMO transition of model **I**. This transition is intrinsically of low intensity, as it involves two $\pi^*\_d_\pi$ orbitals that are perpendicular to each other. The intense band at 650 nm in the UV/Vis spectrum of **2** is assigned to the symmetry- and orbital-allowed $\pi\rightarrow\pi^*$ transition from the $\pi_z^*\_d_{xz}$ orbital (HOMO) to the $d_{xz}\_\pi_z$ orbital (LUMO+1) of **I**. The UV/Vis spectrum of complex **3** exhibits two weak absorptions at 465 (ε = 500 $M^{-1}cm^{-1}$) and 630 nm (ε = 100 $M^{-1}cm^{-1}$), which are assigned to orbital-forbidden ($\pi\rightarrow\sigma$) transitions from the $\pi_y^*\_d_{xy}$ and $\pi_z^*\_d_{xz}$ orbitals (HOMO and HOMO–1) to unoccupied orbitals at the Ti centers. The absorption edge at 380 nm probably results from symmetry- and orbital-allowed $\pi\rightarrow\pi^*$ transitions from the central dinitrogen ligand to the Ti d functions which are therefore at a higher energy than the $\pi\rightarrow\pi^*$ transitions of **1** and **2**.

Discussion

In the preceding section resonance Raman spectra of the moderately activated dinitrogen complexes **1** and **2** were measured and compared with the Raman spectrum of the strongly activated complex **3**. In order to theoretically determine N–N stretching frequencies and evaluate the electronic structure, DFT calculations were performed on structurally simplified models. The UV/Vis spectra of **1/2** and **3** have been interpreted on the basis of the corresponding MO schemes. The N–N stretching frequencies of complexes **1** and **2** were assigned to peaks at 1749 and 1755 cm^{-1}, respectively, which is supported by a DFT frequency calculation predicting the position of this mode at 1806 cm^{-1}. The N–N stretching mode of the strongly activated dinitrogen complex **3**, on the other hand, was identified with a peak at 1284 cm^{-1} in the Raman spectrum, which is supported by a DFT prediction of 1371 cm^{-1} for this mode. The difference in N–N stretching frequency between complexes **1/2** and **3** is thus large (ca. 500 cm^{-1}), which is in agreement with the markedly different N–N bond lengths of these compounds (1.16 Å for **1/2** and 1.29 Å for **3**). The reduction of the N–N stretching frequency of free N_2 at 2231 cm^{-1}[16] to the value observed for complexes **1** and **2** (ca. 1750 cm^{-1}) implies a slight elongation of the N–N bond in these compounds. The N–N stretching frequency of 1284 cm^{-1} found for **3**, on the other hand, corresponds to a significant decrease of the N–N bond order which is comparable to that of a related end-on dinitrogen-bridged zirconium complex for which an N–N stretching frequency of 1211 cm^{-1} and an N–N bond length of 1.30 Å have been determined.[17]

The electronic structure of strongly activated end-on N_2 bridged complexes was described earlier in terms of interactions of dinitrogen π and π* orbitals with metal d_π functions. It was shown that the metal centers primarily interact with the empty π* orbitals of the N_2 to form two metal–dinitrogen π bonding MOs, leading to a significant charge transfer from the metals to this ligand.[18–20] This would agree with the electronic structure of **3** where both π* orbitals of the dinitrogen ligand are occupied (HOMO and HOMO–1), explaining the high degree of activation found for this complex. The electronic structures of the moderately activated complexes **1** and **2** differ from this scheme since only one π* orbital of the dinitrogen ligand is doubly occupied. The two remaining electrons of each titanium center are involved in strong back-bonding interactions with the fulvene ligands and are nonbonding with respect to the bridging dinitrogen ligand. The second π* orbital of the dinitrogen ligand thus remains unoccupied, forming the LUMO of complexes **1** and **2**.

Further information on the electronic structures of **1**–**3** can be inferred from electronic absorption spectroscopy. Inspection of the UV/Vis spectra of **2** leads to the assignment of the 970-nm band to the lowest energy transition of **I**, the HOMO–LUMO transition. On the basis of overlap considerations the intensity of this absorption band should be weak, which is in agreement with the experimental data. The 650-nm transition, on the other hand, is assigned to an electric-dipole-allowed transition from the HOMO to the LUMO+1. In complex **3** the electric-dipole-allowed transitions involving the dinitrogen ligand are located at higher energies. The MO schemes of **I** and **III** further explain the experimental findings that **1**, **2** and **3** are diamagnetic. In model **I**, which exhibits a dihedral angle of about 0° between the Ct*–Ti vectors, the two electrons in the Ti d_{xz} orbitals are strongly coupled via the dinitrogen π^*_z orbital. This is an accurate picture for complex **1** but has to be slightly modified for complex **2**, which exhibits a twisted configuration (dihedral angle between the neighboring Ct*–Ti bonds = 19.1° and 20.0° for the two independent molecules in the asymmetric unit). This reduces the interaction between the two unpaired electrons in the d_{xz} orbitals via the dinitrogen π^*_z orbital, leading in the extreme case, i.e. for a dihedral angle of 90°, to a ferromagnetic coupling (S = 1 ground state).[21] Nevertheless, compound **2** is found to be diamagnetic, i.e. the same as compound **1**, demonstrating that the coupling is predominantly antiferromagnetic (ground state S = 0).

To conclude, the activation of the dinitrogen ligand in **3** is found to be much larger than in **1** and **2**, in contrast to what is expected on the basis of formal oxidation states (Ti^{+}–Ti^{+} for **1** and **2** vs. Ti^{2+}–Ti^{2+} for **3**). It is shown in this paper that this discrepancy can be attributed to the donor/acceptor properties of the set of coligands: whereas **3** has a set of purely electron-donating ligands, strong back-bonding interactions exist between the titanium d orbitals and the fulvene π* orbitals in **1** and **2** which take up four metal d-electrons, preventing them from interacting with the bridging N_2 ligand. This exemplifies once again that the

actual degree of dinitrogen activation in transition-metal complexes depends equally on the set of ancillary ligands and the nature and oxidation state of the metal centers.[22]

Experimental Section

Synthesis of 1, 2, and 3: Compounds **1**,[7] **2**,[7] and **3**[13] were synthesized by literature methods.

Resonance Raman Spectroscopy: Resonance Raman spectra of **1** and **2** were measured with a Dilor XY Raman spectrograph with triple monochromator and CCD detector. An Ar/Kr mixed-gas laser with a maximum power of 5 W was used for excitation. The spectra were recorded with an excitation wavelength of 514.5 nm. The spectra were measured on KBr pellets cooled to 10 K with a helium cryostat. The spectral bandpass was set to 2 cm^{-1}.

Resonance Raman spectra of **3** were measured on a setup involving the following components: Spectra Physics 2020 5 W Ar^+-laser; SPEX 1404 0.85 double monochromator equipped with a CCD camera (PI Instruments, 1024 × 256 pixels EEV chip) and a Peltier cooled RCA 31034 detector connected to a Stanford Research SR 400 photon counter allowing spectra to be recorded in spectrograph or scanning modes; liquid helium cryostat (Cryovac) for measurements from 4.2 to 300 K. The spectra were recorded at 20 K with an excitation wavelength of 514.5 nm and with the spectral bandpass set to 4.5 cm^{-1}.

UV/Vis Spectroscopy: Optical absorption spectra of **2** were obtained from the neat compound pressed between two sapphire plates. The spectra were recorded at 10 K on a Varian Cary 5 UV/Vis/NIR spectrometer. Extinction coefficients were determined by comparison with UV/Vis spectra of **2** in solution. Optical absorption spectra of **3** were obtained from a toluene solution of **3** in an ESR tube. The spectra were recorded with a Bruins Omega10 Spectrophotometer.

Density Functional Theory Calculations: Spin-restricted DFT calculations using Becke′s three-parameter hybrid functional with the correlation functional of Lee, Yang, and Parr (B3LYP)[23–25] were performed for the singlet ground state of model complexes **I** and **III**. Model **I** was optimized in C_1 symmetry. For DFT frequency calculations, model **III** was also optimized in C_1 symmetry, whereas the structure of model **III** used for the single point calculation was derived from the X-ray structure. The LanL2DZ basis set, which applies Dunning/Huzinaga full double-zeta (D95) basis functions[26] on first-row atoms and Los Alamos effective core potentials plus DZ functions on all other atoms, [27,28] was used for the calculations. Convergence was reached when the relative change in the density matrix between subsequent iterations was less than 1×10^{-5} for single points and 1×10^{-8} for optimizations. Charges were analyzed by using the natural bond orbital (NBO) formalism.[29–32] All of the computational procedures were used as implemented in the G98 package.[33] Wave functions were plotted with the visualization program Gaussview 2.1.

Acknowledgments

F. T. thanks DFG Tu58/12-1 and Fonds der Chemischen Industrie for funding this research; R. B. thanks the Fonds der Chemischen Industrie for a scholarship kindly granted to A. S.

[1] M. D. Fryzuk, S. A. Johnson, *Coord. Chem. Rev.* **2000**, *200*, 379.
[2] B. A. MacKay, M. D. Fryzuk, *Chem. Rev.* **2004**, *104*, 385.
[3] S. Gambarotta, J. Scott, *Angew. Chem.* **2004**, *116*, 5412; *Angew. Chem. Int. Ed.* **2004**, *43*, 5293.
[4] C. M. Kozak, P. Mountford, *Angew. Chem.* **2004**, *116*, 1206; *Angew. Chem. Int. Ed.* **2004**, *43*, 1186.
[5] J. Chatt, J. R. Dilworth, R. L. Richards, *Chem. Rev.* **1978**, *78*, 589.
[6] F. Tuczek, N. Lehnert, *Angew. Chem.* **1998**, *110*, 2780; *Angew. Chem. Int. Ed.* **1998**, *37*, 2636.
[7] A. Scherer, K. Kollak, A. Lützen, M. Friedemann, D. Haase, W. Saak, R. Beckhaus, *Eur. J. Inorg. Chem.* **2005**, 1003.
[8] R. D. Sanner, D. M. Duggan, T. C. McKenzie, R. F. Marsh, J. E. Bercaw, *J. Am. Chem. Soc.* **1976**, *98*, 8358.
[9] J. M. deWolf, R. Blaauw, A. Meetsma, J. H. Teuben, R. Gyepes, V. Varga, K. Mach, N. Veldman, A. L. Spek, *Organometallics* **1996**, *15*, 4977.
[10] D. H. Berry, L. J. Procopio, P. J. Carroll, *Organometallics* **1988**, *7*, 570.
[11] J. D. Zeinstra, J. H. Teuben, F. Jellinek, *J. Organomet. Chem.* **1979**, *170*, 39.
[12] T. E. Hanna, E. Lobkovsky, W. H. Bernskoetter, P. J. Chirik, *Organometallics* **2004**, *23*, 3448.
[13] R. Duchateau, S. Gambarotta, N. Beydoun, C. Bensimon, *J. Am. Chem. Soc.* **1991**, *113*, 8986.
[14] N. Beydoun, R. Duchateau, S. Gambarotta, *J. Chem. Soc., Chem. Commun.* **1992**, 244.
[15] S. M. Mullins, A. P. Duncan, R. G. Bergman, J. Arnold, *Inorg. Chem.* **2001**, *40*, 6952.
[16] F. Rasetti, *Proc. Natl. Acad. Sci. USA* **1929**, *15*, 234.
[17] J. D. Cohen, M. Mylvaganam, M. D. Fryzuk, T. M. Loehr, *J. Am. Chem. Soc.* **1994**, *116*, 9529.
[18] C. B. Powell, M. B. Hall, *Inorg. Chem.* **1984**, *23*, 4619.
[19] M. D. Fryzuk, T. S. Haddad, M. Mylvaganam, D. H. McConville, S. J. Rettig, *J. Am. Chem. Soc.* **1993**, *115*, 2782.
[20] R. Ferguson, E. Solari, C. Floriani, D. Osella, M. Ravera, N. Re, A. Chiesa-Villa, C. Rizzoli, *J. Am. Chem. Soc.* **1997**, *119*, 10104.
[21] For some titanium dinitrogen complexes paramagnetic behavior is indeed found: $[(Cp_2Ti)_2\mu\text{-}\eta^1\text{:}\eta^1N_2]$ 1.45 μ_B (300 K); Y. G. Borodko, I. N. Ivleva, L. M. Kachapina, S. I. Salienko, A. K. Shilova, A. E. Shilov, *J. Chem. Soc., Chem. Commun.* **1972**, 1178; $[(Cp^*_2Ti)_2\mu\text{-}\eta^1\text{:}\eta^1N_2]$ 2.18 μ_B (107–298 K); J. E. Bercaw, *J. Am. Chem. Soc.* **1974**, *96*, 5087.
[22] On the basis of the strong back-bonding interaction of the fulvene ligands, it would appear justified to assign a 2– charge to the fulvene ligands. In that case the titanium centers would have a 3+ charge and be able to transfer one electron each to the dinitrogen ligand, making it an N_2^{2-} unit. However, it is customary to treat the fulvene ligands as neutral.
[23] A. D. Becke, *Phys. Rev. A* **1988**, *38*, 3098.
[24] A. D. Becke, *J. Chem. Phys.* **1993**, *98*, 1372.
[25] A. D. Becke, *J. Chem. Phys.* **1993**, *98*, 5648.
[26] T. H. Dunning, Jr., P. J. Hay, in: *Modern Theoretical Chemistry* (Ed.: H. F. Schaefer III), Plenum, New York, **1976**.
[27] P. J. Hay, W. R. Wadt, *J. Chem. Phys.* **1985**, *82*, 270 and 299.
[28] W. R. Wadt, P. J. Hay, *J. Chem. Phys.* **1985**, *82*, 284.
[29] J. P. Foster, F. Weinhold, *J. Am. Chem. Soc.* **1980**, *102*, 7211.
[30] A. B. Rives, F. Weinhold, *Int. J. Quantum Chem. Symp.* **1980**, *14*, 201.
[31] A. E. Reed, R. B. Weinstock, F. Weinhold, *J. Chem. Phys.* **1985**, *83*, 735.
[32] A. E. Reed, L. A. Curtiss, F. Weinhold, *Chem. Rev.* **1988**, *88*, 899.
[33] M. J. Frisch, G. W. Trucks, H. B. Schlegel, G. E. Scuseria, M. A. Robb, J. R. Cheeseman, V. G. Zakrzewski, J. A. Montgomery, Jr., R. E. Stratmann, J. C. Burant, S. Dapprich, J. M. Millam, A. D. Daniels, K. N. Kudin, M. C. Strain, O. Farkas, J. Tomasi, V. Barone, M. Cossi, R. Cammi, B. Mennucci, C. Pomelli, C. Adamo, S. Clifford, J. Ochterski, G. A. Petersson, P. Y. Ayala, Q. Cui, K. Morokuma, P. Salvador, J. J. Dannen-

berg, D. K. Malick, A. D. Rabuck, K. Raghavachari, J. B. Foresman, J. Cioslowski, J. V. Ortiz, A. G. Baboul, B. B. Stefanov, G. Liu, A. Liashenko, P. Piskorz, I. Komaromi, R. Gomperts, R. L. Martin, D. J. Fox, T. Keith, M. A. Al-Laham, C. Y. Peng, A. Nanayakkara, M. Challacombe, P. M. W. Gill, B. Johnson, W. Chen, M. W. Wong, J. L. Andres, C. Gonzalez, M. Head-Gordon, E. S. Replogle, J. A. Pople, *Gaussian 98 Rev. A.11*, Gaussian, Inc., Pittsburgh, **2001**.

Received: August 2, 2005
Published Online: November 15, 2005

